Relaxation and crystallization processes in partially or completely amorphized metallic systems: An ion bombardment study on In_2Au

Thomas Müller and Paul Ziemann*
Abteilung Festkörperphysik, Universität Ulm, D-89069 Ulm, Germany
(Received 15 December 2003; published 30 June 2004)

Polycrystalline In_2Au films prepared by evaporation were bombarded at 4.2 K as well as 80 K with 300 keV Ar^+ ions. In this way, the crystalline phase can be transformed stepwise into an amorphous phase, and by *in situ* controlling the electrical resistance of the films, samples containing well-defined volume fractions of the amorphous phase can be prepared. Performing isothermal temporal relaxation experiments after switching off the ion beam on such samples as well as annealing cycles determining their crystallization temperature T_x, the question could be addressed as to the effect of crystalline nuclei on these properties. A monotonic decrease of T_x is found for an increasing volume fraction of the crystalline phase. The temporal relaxation exhibits a stretched exponential behavior with an exponent pointing to an effective dimension of $d=3$.

DOI: 10.1103/PhysRevB.69.224110 PACS number(s): 61.80.Jh, 72.15.Cz, 61.72.−y, 61.43.Dq

I. INTRODUCTION

Ever since the first experiments demonstrating that quenching a metallic vapor onto liquid-helium-cooled substrates may lead to amorphous phases[1] and, even more so, by the impressive development of the preparation of metallic glasses based on splat cooling their corresponding melts,[2–4] it has become clear that a large variety of binary metallic alloys can be structurally transformed into metastable amorphous phases by various rapid quenching techniques. These amorphous phases quite often exhibit new attractive properties related to their magnetic, optical, mechanical, or superconducting behavior and a series of review papers are dedicated to this fact.[2–6] For the important subclass of metallic glasses showing nearly-free-electron (NFE) characteristics, a close relation has been found between the structure as described by the structure factor $S(k)$, being the Fourier transform of the radial distribution function and its electronic properties characterized by the Fermi wave number k_F. For such amorphous NFE systems, the rather simple criterion $2k_F=k_p$ [k_p designating the position of the first maximum of $S(k)$ in k space] in many cases provides a possibility to determine the stability range $x_{\min}=x=x_{\max}$ of the amorphous phase of a binary alloy $A_{1-x}B_x$.[7,8] For this type of alloy, the relative position of $2k_F$ with respect to k_p is also decisive when calculating the resistivity and its temperature dependence $\rho(T)$. Especially close to the above criterion $2k_F=k_p$ a negative resistance coefficient $(1/R)(dR/dT)$ is theoretically predicted and experimentally observed.[7,9] The underlying theoretical description of the resistance behavior of a NFE amorphous phase plays an important role in the present work dealing with partially or completely amorphized In_2Au alloys, which are known to belong to the NFE systems.[8,10]

For completely amorphous metallic glasses it has already been observed previously that the electrical resistivity ρ changes irreversibly when annealing as-prepared samples within the amorphous phase. Actually, such changes can exhibit both signs, positive[11] as well as negative.[12] Theoretically this phenomenon is attributed to structural relaxation processes within the highly degenerate ground state of the amorphous phase, offering many structural configurations that only slightly differ in energy[13] or, expressed alternatively, in free volume.[14] The resulting changes of the structure factor $S(k)$ can then be related to the observed resistivity according to the above-mentioned Faber-Ziman theory. Closely related relaxation processes, though determined at a fixed temperature, will be studied in the present work for various partially as well as completely amorphized In_2Au films. For that purpose, we exploit the fact that once it is known that a binary system can be amorphized by quenching, it also can alternatively be transformed into the amorphous phase by ion bombardment.[15] In the specific case of In_2Au, this has been already demonstrated previously.[16]

The ion bombardment technique, however, allows us to prepare the amorphous phase in a step-by-step manner by simply increasing the ion fluence ϕ (ions per cm^2) and controlling the resulting amorphization process *in situ* by, e.g., monitoring the ion-induced resistance changes. In this way, partially amorphized samples containing a well-controlled volume fraction of the amorphous phase can be prepared. Thus, isothermal relaxation processes can be studied for the first time, which are observed when interrupting the ion-beam-induced amorphization by switching off the beam while keeping the temperature fixed.

It turns out that a stretched exponential behavior delivers an excellent description of the observed relaxation processes of partially amorphized systems. To arrive at such a good agreement, two processes have to be considered, one of which can be attributed to the still remaining crystalline though defected volume, while the second characterizes irreversible rearrangements within the already amorphized volume fraction. The fluence dependence of the relative weights of these two processes opens the possibility to determine the point when the volume fraction of the amorphous phase becomes dominant as well as when the ion-induced amorphization is practically complete.

A second aspect of the present work is related to the crystallization of the amorphous phase. Since the ion-induced amorphization process allows us to prepare partially amorphized samples in a controlled way, the question can be ad-

dressed as to how the crystalline matrix still present, into which the amorphous phase is embedded, influences the crystallization temperature T_x by providing corresponding nuclei. It will be demonstrated that independent of the chosen projectiles (He^+, Ar^+) or bombardment temperature (4.2 or 80 K), $T_x(c_x)$ increases monotonically when decreasing the volume fraction c_x of the crystalline phase in the sample, approaching a well-defined value $T_x(0)$ for completely amorphized samples with a small transition width $\Delta T_x(0)$.

The approach of $T_x(0)$ when completing the ion-induced amorphization of a sample is accompanied by a continuous decrease of the temperature coefficient $a=(1/R)(dR/dT)$ with a change of sign from positive to negative values about halfway from complete amorphization. Thus, the final amorphous state can be uniquely characterized by a significantly reduced isothermal relaxation towards larger resistances, a maximum crystallization temperature with a minimum transition width and a reversible negative temperature coefficient a of its resistance.

II. EXPERIMENT

Thin In_2Au films (typical thickness 40 nm) were thermally evaporated at ambient temperature onto sapphire substrates using fine granules grinded from a bulk In_2Au sample as starting material. During standard evaporations at a rate of 0.2 nm/s, a pressure of 10^{-7} mbar could be maintainted. The resulting structural as well as stoichiometric properties were determined on selected test films applying x-ray diffraction (XRD) and Rutherford backscattering (RBS) measurements. In all cases, the expected CaF_2 structure with a lattice parameter of 0.65 ± 0.1 nm [bulk value 0.6506 nm (Ref. 17)] as well as the 2:1 stoichiometry (typical experimental error 5%) could be confirmed. After electrically contacting the films for a four-point measurement, they were mounted onto the cold stage of a liquid-helium or -nitrogen irradiation cryostat, respectively, depending on the bombardment temperature T_B of 4.2 or 80 K. In this way, the various irradiation steps corresponding to the total ion fluence ϕ could be combined with an *in situ* determination of the induced resistance changes $\Delta R(\phi)$ at the fixed irradiation temperature.

The irradiations were performed with either He^+ or Ar^+ ions, both of 300 keV. Sweeping the beam horizontally as well as vertically guaranteed a homogeneous irradiation over the exposed film area. A crucial point in the present experiments is the control of the bombardment temperature, which was continuously monitored with and without the ion beam. By reducing the ion current, which also was continuously determined via a Faraday cup, to below 10 nA, the maximum temperature increase due to the ion beam could be restricted to below 2 K at $T_B=4.2$ K and below 0.2 K at $T_B=80$ K. An additional heater mounted on the cold stage allowed us to increase the sample temperature T_S from T_B to 300 K. All significant parameters such as T_S and T_B, the ion fluence ϕ, sample resistance R, and time t could be either controlled or at least continuously monitored via a PC. Thus, the following types of experiments could be performed: $\Delta R(\phi, T_S=T_B=\text{const})$, thereby following up on the ion-induced amorphization process, $\Delta R(\phi=\text{const}, T_S=T_B=\text{const}, t)$, describing the temporal resistance relaxation after switching off the beam, and $\Delta R(\phi_{\max}, T_S)$, giving the annealing behavior after partial or complete amorphization. More details on the ion implanter and the irradiation cryostats can be found elsewhere.[18]

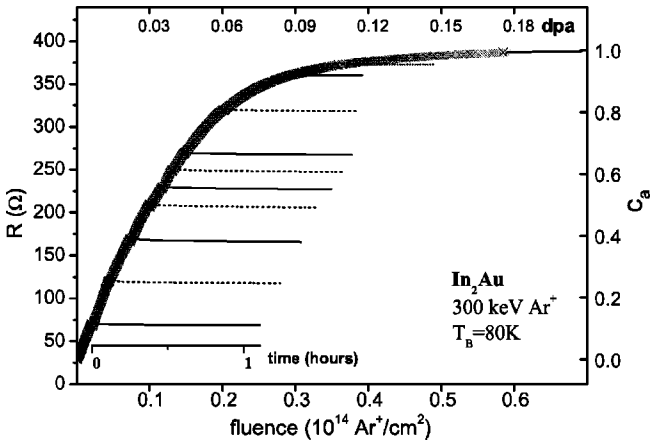

FIG. 1. Amorphization of an In_2Au film as induced by 300 keV Ar^+ bombardment at 80 K. Plotted is the sample resistance versus the ion fluence (lower scale) or the corresponding average displacement per atom (dpa, upper scale). On the right scale, the amorphous volume fraction c_a is given. The horizontal dotted and solid traces give the temporal development of the resistance when interrupting the ion bombardment by switching off the beam.

III. RESULTS AND DISCUSSION

A. Relaxation behavior

The first group of experimental results is related to the relaxation behavior of partly or completely amorphized In_2Au films. In all cases, the sample in its starting condition was polycrystalline and the bombardments were performed at $T_B=80$ K with 300 keV Ar^+ ions. Measuring the ion-induced resistance changes *in situ* allowed us to follow the amorphization process. An example is given in Fig. 1, where the resistance increase (left scale) is plotted versus the ion fluence (lower scale) or, equivalently, versus the average number of displacements per target atom (dpa, upper scale). For instance, a dpa value of 0.2 indicates that, on the average, every fifth target atom has been displaced due to the ion bombardment up to a certain fluence ϕ. In order to extract the dpa value, the average energy deposited by an ion along its track via nuclear collisions must be known together with the displacement energies of the various target atoms. In the present case of In_2Au films bombarded with 300 keV Ar^+ ions, the average nuclear energy loss was calculated with the Monte Carlo program SRIM-2003 (Ref. 19) assuming identical displacement energies of 25 eV for In and Au.

The ion-induced resistance changes shown in Fig. 1 can be nicely described by an exponential saturation behavior $R(\phi)=R_0+\Delta R_{\max}[1-\exp(-B\phi)]$, resulting in the parameter set $R_0=29.1\ \Omega$, $\Delta R_{\max}=379.7\ \Omega$, $B=6.64\times10^{-14}$ cm^2. The absolute value $R_{\max}=R_0+\Delta R_{\max}$ as well as the ratio $R_{\max}/R_0$ agrees excellently with the results found for amorphous and

crystalline In_2Au films prepared by vapor quenching,[20] confirming that amorphization is indeed acquired by the bombardment. As usually, in the following the normalized quantity $c_a(\phi)=\Delta R(\phi)/\Delta R_{\max}$ (right scale in Fig. 1) will be taken as a measure of the amount of amorphous phase present within the sample.[21]

To determine the isothermal relaxation, the ion bombardment was interrupted after certain fluences as illustrated in Fig. 1 and the resistance was monitored as a function of time immediately after switching off the ion beam. The corresponding time axis is included in the figure. As it turned out that the resistance changes due to the structural relaxations involved are of the order of only 2%, they cannot be resolved in the overview of Fig. 1. Before, however, showing these relaxation effects on a magnified scale, it is important to remark on possible temperature effects due to switching the beam on and off the sample. When opening the beam shutter and exposing the total 300 keV beam to the sample holder, which is nominally fixed at 80 K, the thermometer on this holder indicates a temperature increase of only 0.5 K. However, this would not exclude a much higher temperature increase of the thin film sample itself. To measure this value, in the same irradiation cryostat using identical mounting conditions as for the bombardment experiment, the thermal noise of an amorphized film was determined while applying different currents through the sample. In this way it was found that up to 10 mA corresponding to a heating power of 40 mW, the thermal noise did not change, indicating a constant sample temperature. Comparing with the heating power of 3 mW due to the 300 keV ion beam of 10 nA as determined on the sample allows us to safely exclude any significant temperature changes of the sample due to switching the ion beam. After this observation, we now present the resistance relaxation when interrupting the bombardment by switching off the ion beam. For this purpose, in Fig. 2(a) for each interruption, the time dependence of the resistance $R(t)$ normalized to its starting value $R(0)$ is plotted on an extended scale. Presented in this way, the relaxation exhibits a very clear trend. For small volume fractions of the amorphous phase the ion-induced resistance relaxes towards lower values after switching off the beam with maximum values of the order of some percent. Increasing the ion fluence, i.e., the volume fraction of the amorphous phase, leads to a monotonic reduction of the magnitude of this relaxation effect until, at a volume fraction of approximately 75% of the amorphous phase, a change of sign occurs, resulting in a resistance increase due to relaxation processes. The magnitude of this positive effect, though with $<1\%$ being clearly smaller than that in the negative case, continues to increase for larger volume fractions $c_a(\phi)$ and is present also in the completely amorphous phase.

The result presented in Fig. 2(a) suggests a description in terms of two types of processes, one attributed to structural relaxations within the amorphous phase, the other one to the annealing of defects within the still crystalline phase. Within this choice, it appears quite natural to connect the relaxation leading to a resistance decrease to the crystalline phase assuming that bombardment-induced defects in this phase simply anneal out. This is the standard situation in crystalline solids where growing structural disorder always results in a

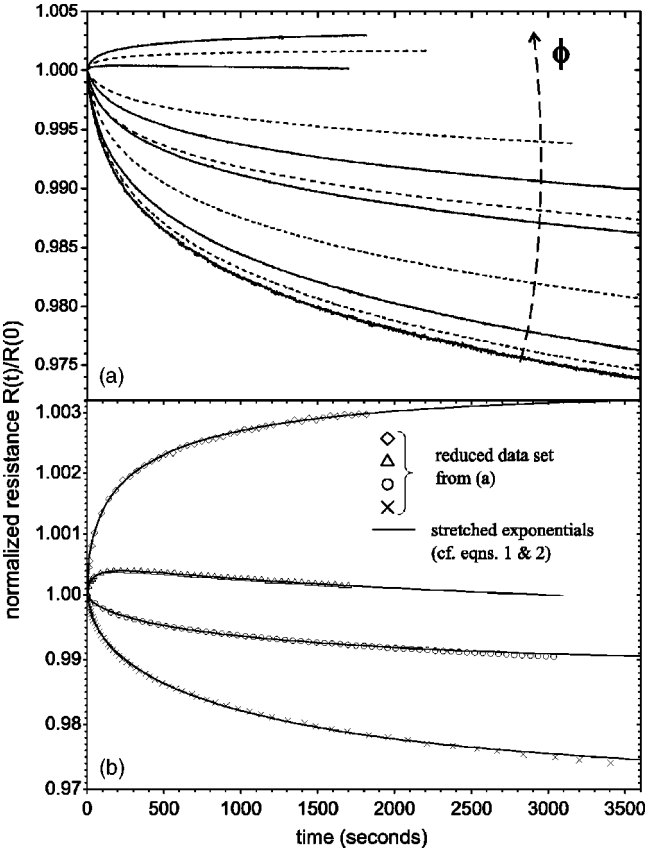

FIG. 2. Temporal relaxation of the electrical resistance of partially and completely amorphized In_2Au samples. (a) Experimental data taken 80 K after switching off the 300 keV Ar^+ beam at the interrupts given in Fig. 1. The arrow indicates the direction of increasing fluences, i.e., increasing amorphous volume fractions. (b) Data sets from (a), reduced in order to make the agreement with fitted stretched exponentials (solid lines) visible.

corresponding resistance increase, while, in the opposite case of reducing disorder a decrease of the resistance is observed. For amorphous solids, however, the situation is not so clear cut. Here, according to Faber-Ziman theory, the response of the resistance to structural changes within the amorphous phase depends on the position of $2k_F$ with respect to k_p as already mentioned above. As a consequence, structural relaxations can lead to an increase or a decrease of the resistance. In the present case, this direction can be additionally tested by thermal annealing the completely amorphized system. For example, starting with a value of $R=391\ \Omega$ for an amorphous In_2Au film at 80 K, the sample was sequentially heated to increasing final temperatures T_f and recooled to 80 K, where the resulting resistance $R_f(80\ \mathrm{K})$ was determined. For the above specific starting value, the following data points were obtained: $R_{90}(80\ \mathrm{K})=393\ \Omega$, $R_{100}(80\ \mathrm{K})=394.5\ \Omega$, $R_{110}(80\ \mathrm{K})=396\ \Omega$, $R_{120}(80\ \mathrm{K})=398\ \Omega$. These data clearly demonstrate that annealing-induced relaxation processes within the amorphous phase lead to increasing resistance values in consistent agreement with what is observed in Fig. 2 for almost and completely amorphized samples after switching off the ion beam. Since in the case of amorphous In_2Au, $2k_F$ approximately matches k_p, one has to

TABLE I. Relaxation parameters of partially and completely amorphized In_2Au films. R_0 is the starting resistance, ϕ is the ion fluence, A_1, τ_1, and p are the fitting parameters for the crystalline volume fraction [cf. Eq. (1)], and A_2, τ_2, q are the fitting parameters for the amorphous volume fraction [cf. Eq. (2)].

R_0 (Ω)	$\phi(10^{13}$ Ar$^+$/cm^2)	A_1	τ_1 (s)	p	A_2	τ_2 (s)	q
70.42	0.21	0.97034	1151	0.581	0		
120.68	0.44	0.9734	965	0.602	0		
169.96	0.73	0.97416	1110	0.586	0		
210.48	1.0	0.979	1150	0.597	0		
230.58	1.17	0.98447	1299	0.580	0		
250.83	1.3	0.98537	1382	0.545	0		
270.31	1.48	0.98877	1346	0.622	0		
320.49	2.0	0.99256	1444	0.594	0		
360.35	2.9	0.99856	7469	0.650	0.00061	60	0.590
372.30	3.6	1			0.00175	226	0.495
386.69	5.9	1			0.00339	379	0.482

conclude, referring to the Faber-Ziman model, that the observed relaxation processes lead to a slight sharpening of the first peak of $S(k)$ with a corresponding increase of its magnitude $S(k_p)$.

The question arises as to how to functionally describe the two types of relaxation processes. While in elemental metals such as Cu, ion and, even more so, electron irradiation leads to well-defined defects such as interstitials or vacancies with characteristic enthalpies of their creation and diffusion,[22] in metallic alloys, the situation is more complicated. Due to local stoichiometry variations and the additional chemical interaction between dissimilar atoms, a variety of defect complexes can be produced by irradiation experiments characterized by a broad distribution of activation energies necessary to make these defects mobile and anneal, resulting in the related resistance relaxation. As a consequence, the time dependence of isothermal annealing in an alloy is not expected to exhibit the typical exponential relaxation behavior characterized by a single time constant as in elemental metals, but should reflect the corresponding broad distribution of time constants. A description in terms of a broad distribution of relaxation time constants should hold even more so for the amorphous phase with its many possible structural configurations resulting in corresponding, almost degenerate ground states. Thus, for both relaxation processes, in the crystalline phase leading to a resistance decrease and in the amorphous phase to a resistance increase, a description appears appropriate taking into account broad distributions of relaxation times. A well-known function adopted especially for such a situation is the "stretched exponential,"[23] currently taken in the following forms:

$$R(t,80\ \mathrm{K})/R(0) = A_1 + (1 - A_1)\exp[-(t/\tau_1)^p], \qquad (1)$$

$$R(t,80\ \mathrm{K})/R(0) = A_2\{1 - \exp[-(t/\tau_2)^q]\}, \qquad (2)$$

where Eq. (1) describes the temporal resistance decrease within the crystalline phase and Eq. (2) the resistance increase in the amorphous phase, both due to structural relaxation processes. Together, Eqs. (1) and (2) give an excellent description of the experimental results as demonstrated in Fig. 2(b) for the two limiting cases of small and large fluences as well as for two fluences in between. The resulting fit parameters A_i, τ_i $(i=1,2)$ as well as p and q are summarized in Table I for the various ion fluences. The exponentials p and q and, similarly, the time constant τ_1 are found to be practically independent of the ion fluence with the average values $p=0.59$, $q=0.49$, $\tau_1=1230$ s, while τ_2, once measurable for higher amorphous volume fractions, shows a trend to increase from 60 s for an 80% amorphous sample to 379 s for a completely amorphized film. Taking the average $\tau_2 = 303$ s, it is clear that the relaxation processes within the amorphous phase are significantly faster than those in the disordered crystalline phase. On the other hand, the "amplitudes" A_i depend on the ion fluence in a way reflecting the trend exhibited by the curves given in Fig. 2(a). The corresponding results are summarized in Fig. 3, where $1-A_1$ (left scale) and A_2 (right scale) are plotted versus the Ar fluence. According to Fig. 2(a), the maximum relaxation towards decreasing resistances is obtained for small ion fluences. The

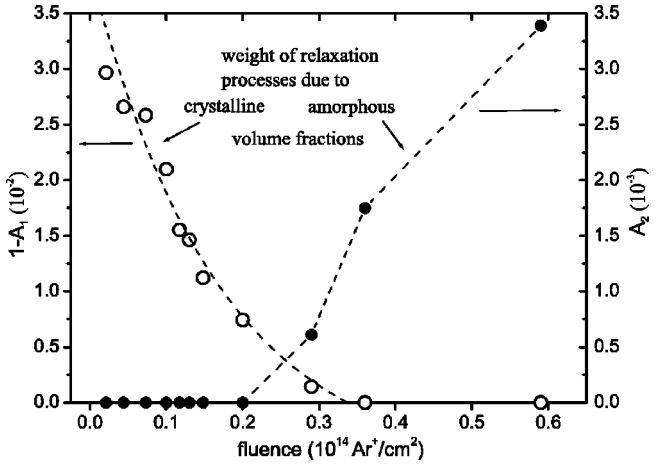

FIG. 3. Different weights of crystalline and amorphous volume fractions to the temporal stretched exponential relaxation processes in partially amorphized In_2Au samples [cf. Eqs. (1) and (2)].

corresponding limiting value for $\phi \to 0$ and $t \to \infty$ is given by $A_1 = 0.965$, i.e., the maximum resistance decrease is 3.5%. On the other hand, for large fluences, i.e., for completely amorphized films, the maximum resistance increase for $t \to \infty$ as given by A_2 is only 0.35%.

In the context of theoretical considerations related to the stretched exponential behavior it is worth noting that both stretching exponents p and q are close to the "magic" value of $3/5 = 0.6$, pointing to relaxation processes in a disordered medium of effective dimension $d = 3$ as concluded from the standard trapping model delivering $p = d/(d+2)$.[23] Remarkably, a stretched exponential behavior with $p = 0.5$ has also been previously reported for the grain growth of nanocrystalline Au films determined via the corresponding resistance changes.[24] Another important point worth mentioning is the fact that up to an amorphous volume fraction of around 80% the relaxation is dominated by the crystalline phase, i.e., resistance decreasing effects with the amplitude A_2 representing processes within the amorphous phase set to zero. This probably is a characteristic of the electric transport measurement, where the well-conducting crystalline phase forms a percolating network dominating the total resistance of the mixture with the much less conductive amorphous phase until this percolation is interrupted at high amorphous volume fractions. The final remark is related to the different fluence dependence of the relaxation times τ_1 and τ_2. A possible explanation may be linked to the expected temperature behavior of t. Assuming a characteristic temperature T_A where certain types of crystalline defects preferentially anneal [for In_2Au such an annealing stage has been found at $T_A = 110$ K (Ref. 25)] and performing the measurements isothermally at $T_B = 80$ K as in the present case, τ should be governed by the ratio T_B/T_A, which is fixed as long as T_A is not dependent on the ion fluence. In the amorphous case, however, the corresponding annealing temperature T_A is identified with the crystallization temperature T_x and, as discussed in the Introduction, it may well depend on the degree of amorphization of a sample, i.e., $T_x(c_a(\phi))$ with its value expected to increase towards complete amorphization. Thus, the ratio $T_B/T_x(c_a(\phi))$ will decrease as a function of the ion fluence, leading to a slowing down of the relaxation processes. In order to support this idea experimentally, in the following section the crystallization behavior of partially as well as completely amorphized samples will be presented.

B. Annealing and crystallization behavior

The experimental procedure is similar to that in the last section. A polycrystalline In_2Au film is bombarded at 80 K with 300 keV Ar^+ ions and the resulting resistance increase is monitored *in situ*. After some distinct fluences, the ion bombardment is interrupted and the sample temperature ramped from 80 to 300 K at a rate of 0.7 K/min while still continuously measuring its resistance behavior. Then, the sample is recooled to 80 K and the ion bombardment continued up to the next total fluence, after which a new annealing cycle is started. These cycles are repeated up to a total ion fluence corresponding to 0.31 dpa, which is significantly higher than the maximum value in Fig. 1, thus guaranteeing

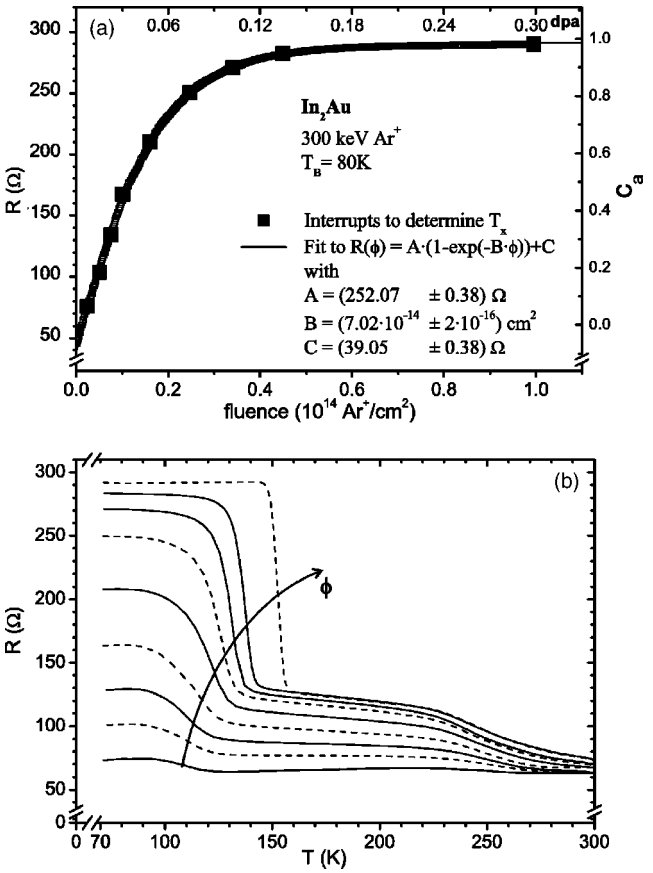

FIG. 4. Annealing behavior of partially and completely amorphized In_2Au samples. (a) Ion-induced amorphization as indicated by the fluence dependence of the resistance (left scale) or of the amorphous volume fraction (right scale). The bombardment interrupts, after which the corresponding annealing behavior as shown in (b) was determined, are indicated by solid squares. The arrow in (b) gives the direction of increasing ion fluences.

complete amorphization of the sample. In this way, the resistance-versus-fluence curve was obtained presented in Fig. 4(a), where the fluences, for which annealing curves have been taken, are marked by solid squares. The corresponding volume fractions of the amorphous phase are indicated by the right vertical scale, while the ion fluences are expressed in dpa by the upper horizontal scale. The exponential saturation behavior $R(\phi) = A[1 - \exp(-B\phi)] + C$ fitted to the experimental data is included in Fig. 4(a) as solid line resulting in the parameters given in the inset.

The annealing curves of the resistance as obtained after the various bombardment interruptions are presented in Fig. 4(b). The stepwise increased fluences at the starting points are reflected by the monotonic increase of the starting resistance values as given in Fig. 4(a). A pronounced irreversible annealing step of the resistance is observed, the height of which is growing with increasing ion fluences and, most important, the temperature position of this step is systematically shifted from 110 K up to 155 K accompanied by a significant sharpening of the transition. The interpretation of this annealing step is very much facilitated by noting that for polycrystalline In_2Au films irradiated with high energetic electrons at 10 K, a prominent, though rather broad recovery

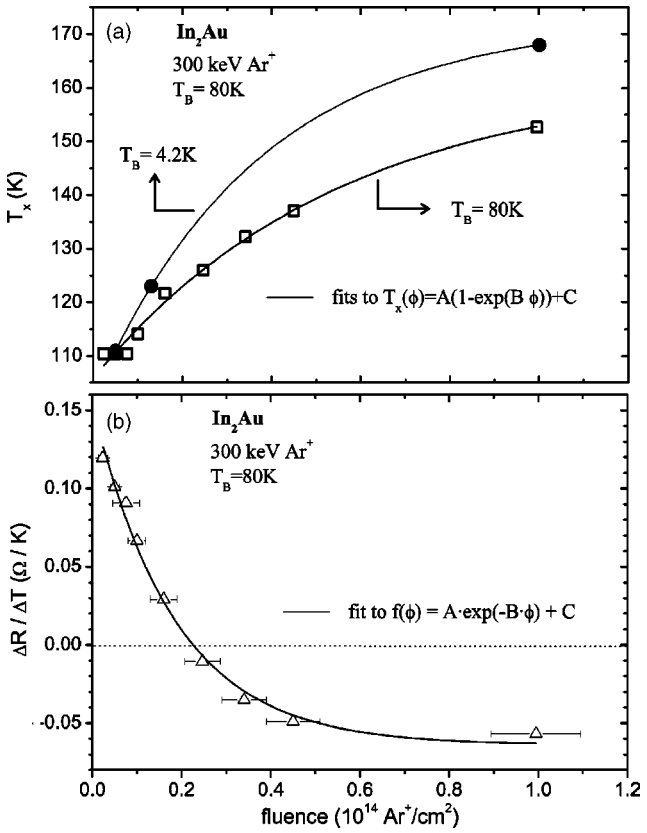

FIG. 5. (a) Crystallization temperatures T_x of In_2Au samples partially or completely amorphized by 300 keV Ar^+ bombardment at 4.2 K (solid dots) or 80 K (open squares), respectively. (b) Slope of the reversible temperature dependence of the resistance as determined between 70 and 80 K for partially or completely amorphized In_2Au samples prior to their crystallization.

step of the irradiation-induced resistance at 100 K has been reported previously[25] and attributed to the recombination of close Frenkel pairs. Accordingly, the annealing steps obtained after small ion fluences (<0.03 dpa) in the present case are similarly attributed to the recovery of defects within the crystalline phase rather than to the crystallization of the very small amount of volume, which already has been amorphized. Within this fluence range, the midpoint temperatures of the annealing steps practically remain fixed at 110 K [cf. Figs. 4(b) and 5(a)]. Additionally, as reported in the last section, for these fluences the relaxation processes related to the amorphous phase still can be neglected ($A_2=0$). Both observations support the above idea of attributing the annealing steps to recovery of crystalline defects. On the other hand, for amorphous In_2Au films crystallization temperatures T_x between 160 and 180 K have been reported[16,20] with the higher values found for films quench-condensed onto liquid-helium-cooled substrates (4.2 K). These crystallization temperatures are in good agreement with the very sharp annealing step at $T_x=155$ K obtained for the highest ion fluence, resulting in a completely amorphized sample. Thus, one is led to attribute the annealing steps observed for ion fluences well above 0.03 dpa to crystallization of the amorphous volume fraction, which, according to Fig. 4(a), monotonically increases as a function of the ion fluence immediately explaining the correspondingly increasing height of the annealing steps. With this interpretation, however, one has to conclude that the crystallization temperatures depend on the volume fraction c_a of the amorphous phase, i.e., $T_x(c_a(\phi))$ with T_x monotonically approaching 155 K, the value of the homogeneous In_2Au amorphous phase. As already argued above in the context of the relaxation processes, the $T_x(c_a(\phi))$ behavior is consistent with the observed fluence dependence of the time constants τ_2, giving additional support to the interpretation of the annealing steps at higher ion fluences.

A final remark may be in order related to a second annealing step visible in Fig. 4(b) at 250 K, i.e., well above the crystallization temperature of the amorphous phase, thus indicating the recovery of defects in the crystalline phase. In the case of electron bombardment, a similar, also quite small, recovery stage has been observed at 200 K, however only for the highest electron energy of 2.5 MeV, but not for 1 MeV or below.[25] Consistently, in the present ion bombardments representing much larger average energy transfers as compared to electrons even for ion energies of only some hundred keV, the stage at 250 K was found in all cases, after Ar as well as He irradiations. This dependence on the energy transferred by the primary collisions points to a type of defect formed within a collision cascade rather than by one single displacement event. Together with the rather high annealing temperature this suggests that the recovery of vacancies or small vacancy clusters can be attributed to the 250 K annealing stage.

We now come back to the first, most pronounced annealing step signaling the crystallization of the amorphous volume fraction. By numerically differentiating the curves given in Fig. 4(b), peaks are obtained, allowing us to position the midpoint temperatures T_x of the annealing steps quite precisely. In this way, the data points of Fig. 5(a) were extracted. While for small fluences (<0.02 dpa) the position of the annealing stage remains practically unchanged at 108 K, the continuous increase observed for larger fluences can be described by an exponential saturation behavior (solid line through the data points), delivering a final value of $T_x=156$ K for the amorphous phase obtained at 80 K.

The stepwise amorphization with successively increasing crystallization temperatures is also reflected in the reversible temperature dependence of the resistance expressed by $\Delta R/\Delta T$ as determined between 70 and 80 K. This is demonstrated in Fig. 5(b), where $\Delta R/\Delta T$ is plotted versus the ion fluence. While for small fluences a positive slope is obtained typical of crystalline metallic samples, which monotonically decreases for increasing fluences until, above $\phi>0.2\times10^{14}$ cm^2 (corresponding to 0.06 dpa), a change of sign is observed saturating for large fluences at $\Delta R/\Delta T=0.064\ \Omega/\mathrm{K}$ as can be extracted from the fitted exponential behavior [solid line through the data of Fig. 5(b)]. Small negative slopes of $\Delta R/\Delta T$ are characteristic of metallic glasses and the above value compares very well with the corresponding results obtained for the quench-condensed amorphous In_2Au phase.[20] Notably, the crossover in sign occurs when the time constant attributed to the amorphous volume fraction becomes dominant as indicated by $A_2\neq0$ (cf. Fig. 3). This *a posteriori* justifies the above assumption that

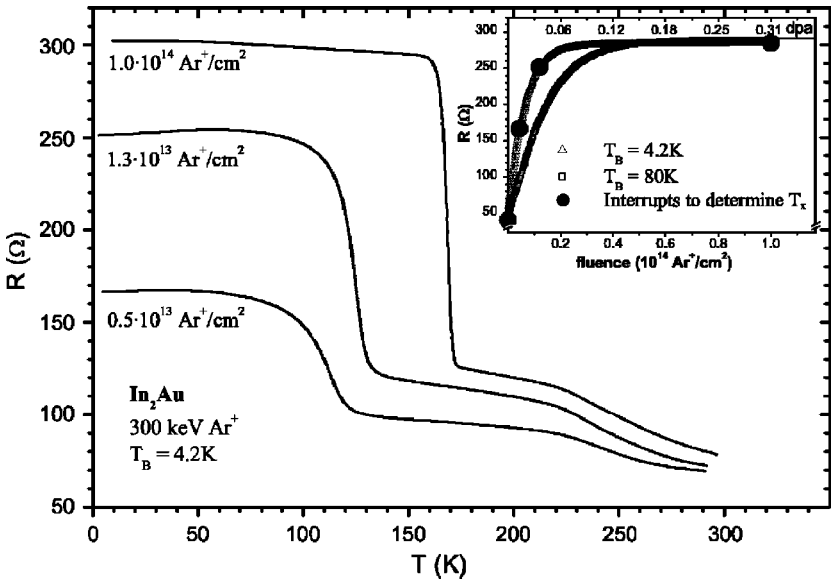

FIG. 6. Annealing behavior of In_2Au samples partially or completely amorphized by 300 keV Ar^+ bombardment at 4.2 K. The corresponding Ar^+ fluences are assigned to each curve. The corresponding amorphization curve $R(\phi)$ is given in the inset, where the related behavior for bombardments at 80 K is included for comparison.

below 0.02 dpa, the ion-induced resistance increases can be attributed to crystalline defects.

The results reported so far were all obtained with the ion bombardments performed at $T_B=80$ K. One might argue, however, that at this temperature with $T_B/T_x \approx 0.5$, significant relaxation processes within the amorphous phase can occur, which then may cause the shift of the crystallization temperatures T_x towards lower values. To exclude such an argument, additional ion bombardments with 300 keV Ar^+ were carried out at $T_B=4.2$ K going through the same experimental procedure as at 80 K, i.e., interrupting the amorphization process at certain fluences and determining the crystallization temperature of the partially amorphized sample, then recooling and continuing the bombardment, and so on. The results obtained in this way for T_x are depicted in Fig. 6. Clearly, the same type of annealing behavior is observed as for $T_B=80$ K with a pronounced step starting at 111 K for the smallest ion fluence and shifting towards 168 K for the highest fluence, in all cases accompanied by a second, much smaller annealing step at 250 K. Thus, the 4.2 K data are completely consistent with those found at 80 K. Correspondingly, the main annealing stage found after 0.03 dpa is attributed to the recovery of crystalline defects, while for higher dpa values >0.03 the crystallization of the amorphous volume fraction $c_a(\phi)$ takes over. Thus, one concludes that the observed monotonous shift $T_x(c_a(\phi))$ towards larger values is an intrinsic property of partially amorphized samples. Obviously, the still existing crystalline volume fraction can provide nuclei allowing the crystallization to occur at a lower temperature. This point can even be put one step further by extracting the midpoint crystallization temperatures from Fig. 6 as before. The results are included in Fig. 5(a) as closed dots and as an exponential behavior fitted to the data. The fact that this curve lies significantly above the 80 K data with an extrapolated saturation value of $T_x=173$ K, in excellent agreement with what is obtained for films quench-condensed at 4.2 K, clearly points to relaxation processes present at 80 K but frozen out at 4.2 K. These processes are also reflected in the resistance buildup during ion irradiation as given by the $R(\phi)$ curves presented in the inset of Fig. 6. At 4.2 K, complete amorphization as indicated by the saturation value of the resistance is reached at a much smaller fluence than at 80 K. On the other hand, the final resistance values are practically indistinguishable. In the context of the T_x behavior, this implies that, for a given quenching rate, it is the preparation temperature of an amorphous phase, which determines the resulting crystallization temperature. When preparing at 4.2 K, practically all thermally activated configurational changes are suppressed and an "ideal amorphous solid"[26] is formed, which, due to the lack of any crystalline nuclei, is the most stable one. In contrast, preparation at 80 K allows the formation of such crystalline nuclei or at least local arrangements having already close similarity to the corresponding short range order of the crystalline phase. This immediately leads to a lowering of the T_x value. Within this interpretation, it is clear that incompletely amorphized samples will exhibit such a T_x depression even more so.

Thus, taking the results of the relaxation as well as crystallization experiments together, a consistent picture emerges. Focusing first on completely amorphized In_2Au films, seemingly identical amorphous phases are obtained by ion bombardment at 4.2 and 80 K, if judged from the corresponding resistivity values. The crystallization temperatures T_x, however, found for these two cases are significantly different pointing to nuclei created at 80 K as opposed to 4.2 K, which then lead to strongly decreased T_x values. The creation of these nuclei may also be involved in the small but clearly observable temporal relaxation of the resistance after switching off the ion beam at 80 K. This type of isothermal relaxation exhibits a stretched exponential behavior with exponents typical of an effective dimension $d=3$. Interpreting the above T_x differences as being due to crystalline nuclei immediately suggests that only partially amorphized samples show even much stronger T_x shifts towards lower values. The experimental results revealing a monotonic T_x enhancement until saturation is reached characteristic of the fully amorphous phase convincingly confirm this conclusion for both bombardment temperatures. Additionally, for partially amor-

phized films the temporal relaxation measurements clearly reveal two contributions, one attributable to the still crystalline and the other to the amorphous volume fraction. Both, however, show a stretched exponential behavior pointing to a broad distribution of relaxation times for the annealing processes and configurational changes involved.

ACKNOWLEDGMENTS

We thank Dr. H.-G. Boyen and Dr. A. Plettl for valuable discussions and technical advice. Support by the Deutsche Forschungsgemeinschaft (GRK 328) is gratefully acknowledged.

*Electronic address: paul.ziemann@physik.uni-ulm.de

[1] W. Buckel and R. Hilsch, Z. Phys. **138**, 109 (1954).
[2] H.-J. Güntherodt and H. Beck, *Glassy Metals I, Vol. 46 of Topics in Applied Physics* (Springer Verlag, Berlin, 1981).
[3] H.-J. Güntherodt and H. Beck, *Glassy Metals II, Vol. 53 of Topics in Applied Physics* (Springer Verlag, Berlin, 1983).
[4] H.-J. Güntherodt and H. Beck, *Glassy Metals III, Vol. 72 of Topics in Applied Physics* (Springer Verlag, Berlin, 1994).
[5] K. Samwer, Phys. Rep. **161**, 1 (1988).
[6] T. Egami, Rep. Prog. Phys. **47**, 1601 (1984).
[7] P. J. Cote and L. V. Meisel, in *Glassy Metals I*, edited by H.-J. Güntherodt and H. Beck (Springer Verlag, Berlin, 1981), p. 141.
[8] P. Häussler, Phys. Rep. **222**, 65 (1992).
[9] S. R. Nagel, Phys. Rev. B **16**, 1694 (1977).
[10] H.-G. Boyen, R. Gampp, P. Oelhafen, B. Heinz, P. Ziemann, C. Lauinger, and S. Herminghaus, Phys. Rev. B **56**, 6502 (1997).
[11] E. Balanzat and J. Hillairet, J. Phys. F: Met. Phys. **11**, 1977 (1981).
[12] S. Takamura and M. Kobiyama, Radiat. Eff. Lett. Sect. **86**, 43 (1984).
[13] A. Heuer, Phys. Rev. Lett. **78**, 4051 (1997).
[14] P. Allia, R. Sato Turtelli, and F. Vinai, Solid State Commun. **43**, 821 (1982).
[15] P. Ziemann, Mater. Sci. Eng. **69**, 95 (1985).
[16] W. Miehle, A. Plewnia, and P. Zieman, Nucl. Instrum. Methods Phys. Res. B **59/60**, 410 (1991).
[17] J. P. Goral and L. Eyring, J. Less-Common Met. **116**, 63 (1986).
[18] A. Plewnia, B. Heinz, and P. Ziemann, Nucl. Instrum. Methods Phys. Res. B **148**, 901 (1999).
[19] J. F. Ziegler, J. P. Biersack, and U. Littmark, *The Stopping and Range of Ions in Solids* (Pergamon, New York, 1996).
[20] P. Häussler, Z. Phys. B: Condens. Matter **53**, 53 (1983).
[21] C. Jaouen, J. Delafond, and J. P. Rivière, J. Phys. F: Met. Phys. **17**, 335 (1987); resistance as a measure for damaged volume.
[22] W. Schilling, G. Burger, K. Isebeck, and H. Wenzl, in *Vacancies and Interstitials in Metals*, edited by A. Seeger, D. Schumacher, W. Schilling, and J. Diehl (North-Holland, Amsterdam, 1969).
[23] J. C. Phillips, Rep. Prog. Phys. **59**, 1133 (1996).
[24] J. Ederth, L. B. Kish, E. Olsson, and C. G. Granqvist, J. Appl. Phys. **91**, 1529 (2002).
[25] I. Eppler, U. Dedek, F. Dworschak, and W. Schilling, J. Phys.: Condens. Matter **10**, 4195 (1998).
[26] Z. H. Stachurski, Phys. Rev. Lett. **90**, 155502 (2003).